OENO One
VINE AND WINE OPEN ACCESS JOURNAL
By IVES International Viticulture & Enology Society

DOI: https://doi.org/10.20870/oeno-one.2023.57.2.7441

OPEN ACCESS

ORIGINAL RESEARCH ARTICLE

Projected impacts of climate change on viticulture over French wine regions using downscaled CMIP6 multi-model data

Sébastien Zito[1,2], Julien Pergaud[3], Yves Richard[3], Thierry Castel[3], Renan Le Roux[4], Iñaki García de Cortázar-Atauri[4], Hervé Quenol[5] and Benjamin Bois[3,6]

[1] UMR 1287 Ecophysiologie et Génomique Fonctionnelle de la Vigne – INRAE, ISVV, 210, chemin de Leysotte, 33882 Villenave d'Ornon, France
[2] Service Recherche & Développement, Maison Hennessy, rue de la Richonne, 16101 Cognac, France
[3] Biogéosciences, UMR 6282 CNRS, université de Bourgogne, 6 boulevard Gabriel, 21000 Dijon, France
[4] INRAE, US 1116 AgroClim, 84914, Avignon, France
[5] UMR6554 LETG-Rennes, Université Rennes 2, Place du Recteur Henri Le Moal, 35043 Rennes Cedex
[6] IUVV, Université Bourgogne-Franche-Comté, 2 rue Claude Ladrey, 21000 Dijon, France

This article is published in cooperation with the 22nd GiESCO International Meeting, hosted by Cornell University in Ithaca, NY, July 17-21, 2023.

Guest editors: Laurent Torregrosa and Stefanos Koundouras.

*correspondence:
sebastien.zito@inrae.fr

Associate editor:
Laurent Jean-Marie Torregrosa

Received:
27 February 2023

Accepted:
18 April 2023

Published:
20 June 2023

ABSTRACT

Climate change is a major challenge for the French wine industry. Climatic conditions in French vineyards have already changed and will continue to evolve impacting viticulture.

This study aims to analyse the evolution of agro- and eco-climatic indices based on phenology simulation of French wine-growing regions. This evolution was analysed on a recent-past period (1962–1991 to 1992–2021) using SAFRAN climate data and on a future projected period (1985–2014 to 2041–2070) with two SSP trajectories (SSP2-4.5 and SSP5-8.5). A set of 19 CMIP6 climate models downscaled at 8 km grid resolution over France coupled with three phenological and a water balance model were used. Phenological model parameters and training system characteristics were adapted to each region to match as much as possible current practices.

Temperatures during the growing season have increased by +1 °C to +2.1 °C since the second half of the 20th century and could rise to +3.7 °C in regions around the Mediterranean by 2070. The inter-model variance concerning the precipitation is high, a significant change (decrease) in precipitation during the grapevine growing season is observed only for the regions of western France (Oceanic climate) over the period 2040–2071 with the SSP5 trajectory. All simulated phenological stages have shifted toward earlier dates. Their occurrence should be even earlier by 2070 with an average advance of up to 22 days for the mid-veraison of Pinot noir in eastern France. The theoretical maturity date (sugar content) should also be advanced from 19 to 30 days depending on the considered region and SSP. Thermal conditions closer to the photosynthetic optimum should promote onset by the early second half of the 21st century. The increase in both the number of hot days and grapevine water deficit during the period of fruit development should impact grape production in quality and quantity in all wine-growing regions. Spring frost projections show no significant change in risk for the second half of the 21st century, compared to current conditions.

KEYWORDS: phenology, ecoclimatic indices, agroclimatic indices, grapevine

INTRODUCTION

Winegrape is a crop for which the quality and the identity of the final product depend strongly on the climatic conditions of the region and the year. By impacting production systems and how wines are developed, climate change represents a major challenge for the wine industry (Ollat *et al*., 2021).

Phenology can be considered a major biological indicator of climate change (Menzel *et al*., 2006). Studies on the evolution of the main phenological stages of the vine with climate change, in New Zealand (Ausseil *et al*., 2021), USA (Wolfe *et al*., 2005), Europe (Jones *et al*., 2005) and France (García de Cortázar-Atauri *et al*., 2017), are mainly concerned with budburst, flowering, veraison as well as harvest, considered as a proxy for the moment when the grapes have reached maturity.

A recent review (Droulia and Charalampopoulos, 2021) listed 29 publications using climate projected data (most of them with CMIP5 downscaled climate data) to simulate grapevine phenology, yield or bioclimatic indices potential evolution in different European wine growing regions or for the European viticulture as a whole. The large majority of these studies focus either on the evolution of phenology phases or bioclimatic indices without considering them together. Recent studies by Morales-Castilla *et al*. (2020) and Sgubin *et al*. (2023) consider changes in phenological timing to calculate bioclimatic indices and grapevine response to projected climate change. However, these studies do not account for each region-specific training system and cultivar. These differences may affect grapevine phenology and water status.

In 2021, France is the second largest country in the world regarding planted vineyards areas (797,600 ha) and the second largest wine producer (more than 37 million hl; OIV statistics). The French vineyards are divided into a large number of wine-growing regions characterised by different climates, cultivars and vine training systems impacting the typicality of the wine produced. Thus French vineyards have been and will be impacted by climate change in various ways, with greater or smaller differences between wine regions.

The purpose of this study is to use a large statistically downscaled CMIP6 climate database (19 models on an 8 km grid) over France covering the 1960–2100 period with two Shared Socio-Economic Pathways (SSP2 and SSP5) to (i) calculate agroclimatic indices during the growing season; (ii) simulate the evolution of grapevine phenology and grape maturity evolution using 8 cultivars; (iii) calculate the evolution of ecoclimatic indices based on simulated

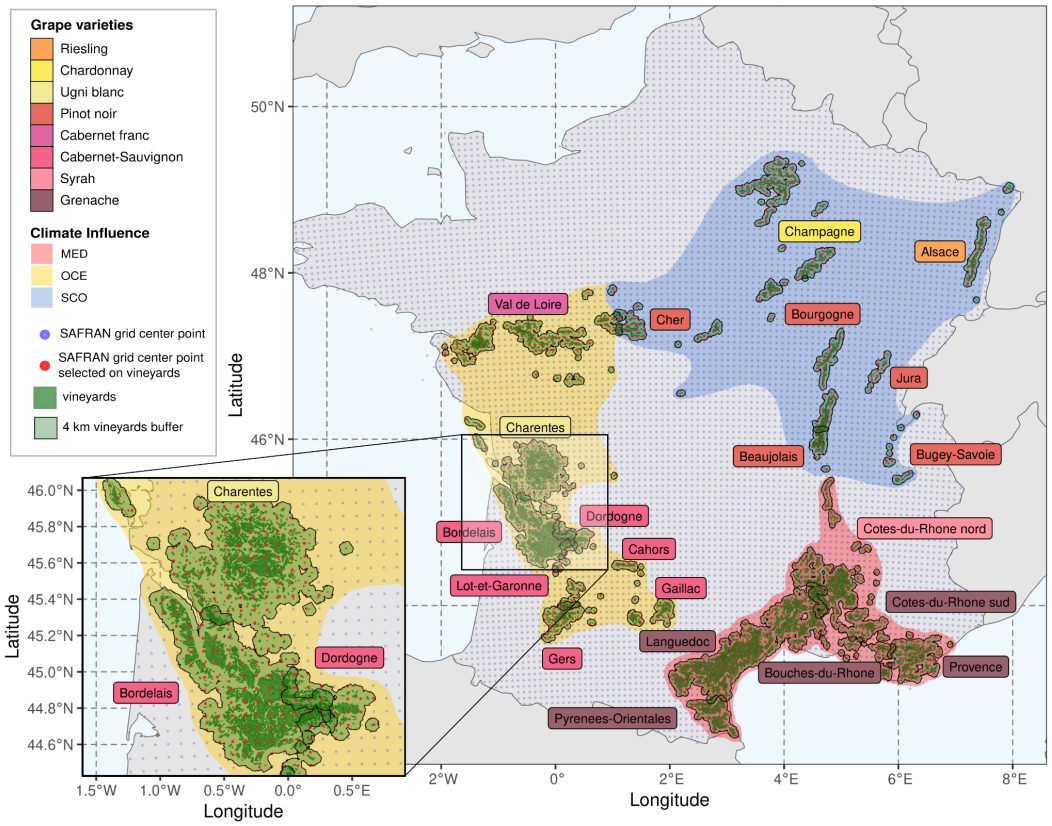

FIGURE 1. French wine regions identified using the Corine Land Cover database, including a 4 km buffer. Each region belongs to a distinct zone defined by the major climatic type in the wine region: Oceanic (OCE), Semi-Continental Oceanic (SCO) and Mediterranean (MED). All SAFRAN grid centre points within the buffer zone (in red on the figure) are selected. All different grape varieties selected (see after Table 1) are represented on the map by the colour of the boxes for each wine region.

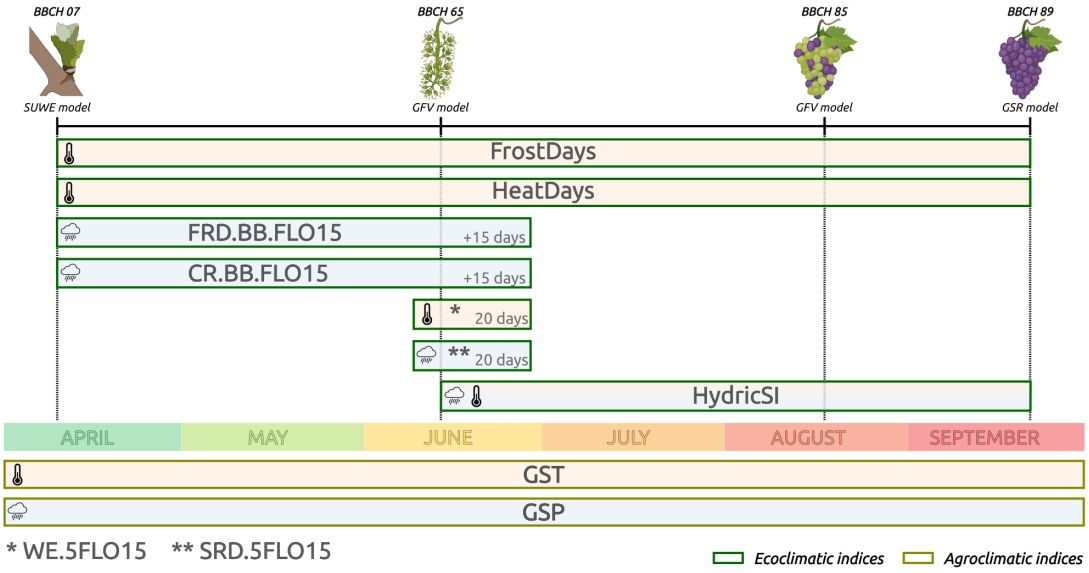

FIGURE 2. Diagram representing the different ecoclimatic indices (depending on the plant phenological stages) and agroclimatic indices (based on the calendar to represent the growing season).

phenology for each of the 21 wine-growing regions identified in France.

The modelling approach used here integrates the fact that different varieties and different training systems are used in French wine regions.

A set of robust phenological models and water balance modelling validated in the context of viticulture were used to integrate the response of phenological features of regional cropped varieties at the present French wine region scale. This allows us to visualise the direct impact that climate change could have on plant growth, frost risk, water deficit, disease risk and the potential maturity of the grapes.

MATERIALS AND METHODS

1. Climate data

Observed climate data came from the SAFRAN (Système d'Analyse Fournissant des Renseignements Adaptés à la Nivologie) database produced by the French national weather service (Meteo-France). Daily minimum and maximum temperature and precipitation at an 8 km resolution grid from 1960 to 2021 were extracted over the French wine-growing regions. A total of 21 wine-growing regions were defined (Figure 1), based on the digitalized and geo-referenced map of the French wine-growing basins (Simonovici, 2019), and using an identification of the areas planted with vines provided by the Corine Land Cover (CLC) database from Copernicus land cover products (https://land.copernicus.eu/pan-european/corine-land-cover/clc2018).

SAFRAN grid cells representative of vineyard areas were selected with a 4 km buffer zone around CLC vineyard polygons (Figure 1). Derived from a simplification of the French climate type from Joly *et al.* (2010), three classes of dominant climatic influences had been established to characterise wine-growing regions: Mediterranean (MED), oceanic influence (OCE) and Semi-Continental Oceanic (or degraded oceanic; SCO).

Climate projections came from general circulation models (GCMs) of the CMIP6 exercise (Coupled Model Intercomparison Project; Eyring *et al.,* 2016) with two Shared Socio-Economic Pathways SSP2-4.5 (call after SSP2) and SSP5-8.5 (call after SSP5). In total, data from 19 GCMs (listed in supplementary data) were statistically downscaled and debiased to SAFRAN's 8 km resolution grid using the quantile mapping method (Gudmundsson *et al.,* 2012). Details of the downscaling process and the assessment of the quality of the resulting climate data are presented in Zito's PhD thesis (2021). The evolution of a set of indices is carried out over two main periods: (i) a recent-past period based on SAFRAN data by comparing the average between 1962–1991 to 1992–2021 and (ii) a future projected period by comparing 1985–2014 and 2041–2070 periods (CMIP6 models).

2. Bioclimatic indices

Several bioclimatic indices were calculated. They consist either of indices calculated on fixed calendar dates (so-called hereafter *agroclimatic indices*) or indices calculated on periods relative to phenological stages (so-called hereafter *ecoclimatic indices* (Caubel *et al*., 2015), hence changing from year-to-year (Figure 2).

Regarding the simulation of phenology stages, three phenological models were used to simulate the budburst (combination of the Smoothed-Utah model, to simulate dormancy break by accumulating chilling units and Wang and Engel model, to simulate the postdormancy phase until budbreak, hereafter referred as SUWE; Morales-Castilla *et al*., 2020), flowering and veraison (GFV: Parker *et al*., 2011) and theoretical maturity (i.e., the date when a given sugar content in grapes is reached, GSR: Parker *et al*., 2020). Six grape varieties were selected according to the wine region with different concentrations of sugar for theoretical maturity (Figure 1 and Table 1).

TABLE 1. Phenological (grape variety and maturity sugar content) and soil water balance (canopy height and width, distance between rows) models parameters selected for each wine-growing region of France. In Champagne and Cognac, theoretical maturity was set at 170 g/L, which is a value commonly reached at harvest to produce sparkling wines and base wine for brandies.

Climate influence	Cultivar	Wine-growing Regions	Maturity sugar content [g/L]	Canopy height [m]	Canopy width [m]	Distance between rows [m]	Comments
Semi-Continental and Oceanic	Riesling	Alsace	190	1.5	0.4	2	Very high rows in Alsace. 190g/L of sugar equivalent to 11.2° of alcohol which is observed in the early 2000s (Duchène *et al.*,2005)
	Chardonnay	Champagne	170	0.8	0.4	1	Sparkling Chardonnay
	Pinot noir	Bourgogne	210	0.8	0.4	1	Classical Burgundy cultivar (Côte de Nuits)
		Beaujolais	210	0.8	0.4	1.5	No parametrization is available for Gamay's budburst. Pinot noir which is cultivated in Beaujolais is used
		Jura	210	1.5	0.4	2	Chardonnay would be more adapted, but no parameter for 210 g/L
		Bugey-Savoie	210	1.2	0.4	2	Presence of Pinot noir in Savoie and Bugey
		Cher	210	0.8	0.4	1	Red Sancerre is made with Pinot noir
Oceanic	Cabernet franc	Val de Loire	210	1.2	0.4	2	Regular Val de Loire appellation
	Ugni blanc	Charentes	170	1.2	0.4	2	Very large majority of Ugni blanc for Cognac production
	Cabernet-Sauvignon	Bordelais	210	1.2	0.4	2	Regular Bordeaux appellation
		Dordogne	210	1.2	0.4	2	Bergerac type
		Lot-et-Garonne	210	1.2	0.4	2	Not representative, but local cultivars are not represented in phenological models
		Gers	210	1.2	0.4	2	
		Cahors	210	1.2	0.4	2	Cabernet-Sauvignon is chosen because it can be cultivated there. Poor calibration of Cot (Malbac) for GSR.
		Gaillac	210	1.2	0.4	2	
Mediterranean	Syrah	Côtes-du-rhône Nord	210	1	0.4	2	Typical variety for Hermitage
	Grenache	Côtes-du-rhône Sud	210	1.2	0.4	2	Southern Rhône appellation in VSP (no gobelet)
		Bouches-du-Rhône	210	1.2	0.4	2	Same configuration to all mediterranean wines: Grenache and 2m row spacing
		Provence	210	1.2	0.4	2	
		Languedoc	210	1.2	0.4	2	
		Pyrénées-Orientales	210	1.2	0.4	2	

Agroclimatic indices are calculated here on the April–September period (Figure 2), which seems to be more closely adjusted to the vegetative season for the French vineyards than the April–October period as proposed by Jones (2003):

- modified growing season average temperature (mGST; April to September);

- modified growing season cumulative precipitation (mGSP; April to September);

Based on simulated phenological stages a set of seven indices were calculated:

- FrostDays: the number of days with temperature below 0 °C from budburst to harvest;

- HeatDays: the number of days with temperature over 35 °C from budburst to harvest;

- FRD.BB.FLO15: the frequency of days with precipitation > 1 mm from budburst to 15 days after mid-flowering. We assume that this is the period during which most of the mechanisation, constrained by rainy days) for weeding and spraying is performed;

- CR.BB.FLO15: the cumulative precipitations from budburst to 15 days after mid-flowering, as rainfall favours Downy mildew and black rot during this period during which grapevine is highly sensitive to contaminations;

- SRD.5FLO15: the number of days with precipitation > 1 mm from 5 days before to 15 days after the

mid-flowering stage. Rain events during this crucial period are detrimental to pollination and fruit set;

- WE.5FLO15: the average value from 5 days before to 15 days after the mid-flowering stage of thermal effect on grapevine development using the equation of Wang and Engel, a bell-shaped curve providing a response from 0 (no effect beyond 0 and 40 °C) to 1 (optimum, fixed at 27.6 °C) following García de Cortázar-Atauri *et al*. (2010) optimization for cv. Pinot noir which is consistent with the photosynthetic optimum of grapevine;

- HydricSI stress index from mid-flowering to harvest. This hydric stress index corresponds to 1 - average of daily relative stomatal conductance of grapevine between flowering and maturity. Relative stomatal conductance (varying from 0 to 1) is calculated using Lebon's soil water balance model (Lebon *et al*., 2003), with a soil water capacity set at 150 mm (supposedly filled every January 1st of each year) for all regions and canopy parameters set to represent a common training system in each region (Table 1). The grapevine growth was simulated with a degree days model coupled with Riou *et al*. (1989) vine rows and soil radiation interception model. Parameters for row porosity and azimuth are fixed at 25 % and 0°, respectively, for all regions.

Phenological and theoretical maturity modelling were performed selecting only one grape variety per wine region, which helped to synthesise results. We tried to select a more or less representative planted grape variety in each region, knowing that it also had to be parameterized for phenological and maturity models. In total, eight different grape varieties were selected (Table 1). The selected variety was not always the most cultivated in each region. First, while GFV models offer parameters for a large number of cultivars, SUWE provides parameters for 12 varieties. As for GSR, it provides heat requirements for numerous (65) varieties but the target grape sugar concentration value may change from one variety to another. GSR target sugar concentration was set up based on the current (early 21st century) practices observed in each region. It was generally set up to 210 g/L (i.e., 21.5 Brix and 12.5 % vol. of potential alcohol in wines) for most regions producing still wines. However, this value was set up at 190 g/L in Alsace, to match values reported by Duchène and Schneider (2005).

The current sugar value at which grapes are picked is very likely underestimated because growers take advantage of warmer conditions to pick grapes at greater levels of ripeness, as observed in Bordeaux wineries or Southern France (van Leeuwen and Destrac-Irvine, 2017). However, note that GSR parameters for greater values of sugar content are restricted to a limited number of cultivars, and the highest retained value was 210 g/L.

During cool vintages, occurring frequently during the 20th century, the heat units required to reach theoretical maturity might never be reached. In this situation, the harvest date was forced on November 1st. One particularity concerns the Cabernet franc selected for the Val de Loire region, whose parametrization for budburst is not set in the SUWE model, Merlot was used instead for parameterization (for budburst only). Merlot is cultivated in the region and has a very similar date of budburst compared to the Cabernet franc.

3. Significant evolution determination

The characterization of the significant evolution of all bioclimatic indices and phenological phases in each of the wine-growing regions considered over the different periods is carried out according to the five following steps:

- calculation of the indices on all selected grid cells;

- use of a statistical test (parametric/non-parametric) for comparing mean differences between periods for each of the grid cells within the wine regions;

- calculation of the average (30 years) of the grid cells in each wine region for each of the indices;

- in the case of historical data (1962–1991 and 1992–2021), attribution of a significant change in the indices when more than 50 % of the grid cells in the region show a significant difference;

- in the case of data for the period 2041–2070, attribution of a significant change in the index when more than 50 % of the climate models have more than 50 % of the region's grid cell with a significant difference.

For projected climate data, we used the median expressed in terms of the difference between the simulation over the reference period (1985–2014) and the future period (2041–2070). The standard deviation over GCMs is used to express inter-model variability.

RESULTS

1. Bioclimatic indices

A significant increase in temperature during the growing season (mGST) in all French wine-growing regions was observed between the periods 1962–1991 and 1992–2021 (Table 2). The regions in the east/northeast of France, under SCO influence, are the most affected by the recent warming. Beaujolais shows the largest increase (+2.1 °C), followed by Champagne and Alsace (+1.5 °C and +1.4 °C, respectively). Regions under OCE influence such as Charentes (+1 °C) and Dordogne (+1 °C) had the smallest, but still significant, increases. Regarding cumulative rainfall from April to September (mGSP) no significant change is observed between the two past periods (1962–1991 and 1992–2021).

Projections for the middle of the 21st century reveal a significant net increase in temperature during the growing season for all wine regions, amplified with SSP5 (Table 3). The MED regions would be the most affected by the increase in mGST (+2.4 °C to +3.7 °C on average according to the SSP). OCE and SCO regions have similar projected evolution with a mean of +1.8 °C and +2.5 °C with SSP2 and SSP5. In terms of cumulative precipitation during the growing season, no significant change is observed in the majority of CMIP6 models used with the SSP2. However, a significant decrease is observed in all OCE regions (–61 mm on average; Table 3).

TABLE 2. Evolution of bioclimatic indices and phenology over the past-present period (SAFRAN data). Values correspond to average differences between the 1962–1991 and 1992–2021 periods averaged over wine regions. Values with * indicate the presence of a significant difference between the two periods for at least half of the SAFRAN grid cell selected in each region.

Climate influence	Cultivar	Wine-growing Regions	mGST [°C]	mGSP [mm]	BUD [doy]	FLO [doy]	VER [doy]	MAT [doy]	FrostDays [days]	HeatDays [days]	FRD.BB.FLO15 [%]	CR.BB.FLO15 [mm]	SRD.5FLO15 [days]	WE.5FLO15 [unitless]	HydricSI [unitless]
Semi-Continental and Oceanic	Riesling	Alsace	1,40*	-1	-8*	-10*	-16*	-17*	-0.8	0	-2.4	-7.1	-0.5	0.05*	-0.017
	Chardonnay	Champagne	1,50*	9	-9*	-10*	-18*	-21*	-0.8	1	-2.4	-7.9	-0.7	0.042	-0.013
	Pinot noir	Bourgogne	1,30*	7	-7*	-9*	-13*	-16*	-0.2	1	-1	-1.1	0.1	0.042*	0.005
		Beaujolais	2,10*	-8	-12*	-14*	-21*	-26*	-0.6	1	0.3	-8	1.2	0.045*	0.008
		Jura	1,00*	17	-6*	-8*	-12*	-13*	0	0	-2.3	-9.9	-0.4	0.033	0.003
		Bugey-Savoie	1,40*	29	-9*	-10*	-17*	-18*	-0.8	0	-0.9	-2.5	0.2	0.041	0.009
		Cher	1,30*	24	-8*	-9*	-14*	-17*	-0.6	1	-0.8	6.5	0.3	0.04	0.01
Oceanic	Cabernet franc	Val de Loire	1,10*	17	-9*	-8*	-13*	-14*	-0.1	0	0.6	17.8	0.6	0.044*	-0.017
	Ugni blanc	Charentes	1,00*	1	-6*	-7*	-11*	-11*	0	0	0.5	7.4	0.3	0.033	-0.007
	Cabernet-Sauvignon	Bordelais	1,20*	16	-7*	-8*	-11*	-13*	-0.4	0	0.7	19.3	0.9	0.046*	0.019
		Dordogne	1,00*	33	-6*	-7*	-10*	-11*	-0.2	0	1.8	30.1	1.1	0.043*	0.025
		Lot-et-Garonne	1,30*	18	-8*	-9*	-12*	-14*	-0.1	0	0.8	20.5	0.8	0.04*	0.002
		Cahors	1,40*	28	-7*	-9*	-13*	-16*	-0.1	2*	0.1	20.1	0.7	0.051*	-0.046
		Gers	1,40*	15	-9*	-9*	-13*	-15*	-0.3	0	-0.1	8.5	0.6	0.045*	0.01
		Gaillac	1,10*	19	-5*	-7*	-10*	-12*	0.1	2*	-0.1	13.5	0.7	0.036	-0.034
Mediterranean	Syrah	Côtes-du-rhône Nord	1,40*	22	-8*	-10*	-15*	-16*	-0.3	1	0.4	6.9	0.8	0.033	0.005
	Grenache	Côtes-du-rhône Sud	1,40*	25	-7*	-8*	-12*	-13*	-0.2	2*	1.7	14.3	0.3	0.035*	-0.042
		Bouches-du-Rhône	1,30*	27	-4*	-6*	-10*	-12*	0	1	1.7	18.4	0.2	0.038*	-0.063*
		Provence	1,30*	18	-4*	-6*	-9*	-12*	-0.1	2	1.7	21.7	0.6	0.036*	-0.041
		Languedoc	1,30*	25	-5*	-7*	-10*	-12*	0	2	1.9	16.6	0.4	0.03*	-0.054
		Pyrénées-Orientales	1,10*	1	-4*	-6*	-9*	-10*	0	1	1.7	12.9	0.2	0.023	-0.048
All regions average			1.3*	17	-7*	-8*	-12*	-14*	-0.2	0.9	0.7	12	0.4	0.038*	-0.022

BUD = budburst; FLO = mid-flowering; VER = véraison; MAT = theoretical maturity; mGST = April-to-Sept. average temperature; mGSP = April-to-Sept. precipitation; FrostDays = count of days with min. temperature below 0 °C after budburst; HeatDays: count of days with max. temperature over 35 °C between BUD and MAT; FRD.BB.FLO15 = frequency of days with precipitation from BUD to 15 days after FLO; CR.BB.FLO15 = precipitation from BUD to 15 days after FLO; SRD.5FLO15 = count of days with precipitation 5 days before to 15 days after FLO; WE.5FLO15 = average heat units calculated daily with the Wang-and-Engel function, 5 days before to 15 days after FLO; HydricSI = stress index corresponds to 1 - average of daily relative stomatal conductance of grapevine between flowering and maturity.

All other regions also exhibit a decrease in precipitation during the growing season but with a higher variability between models suggesting limited confidence in this result.

2. Phenology

Concerning the phenological stages (Table 2), whatever the grape variety or wine-growing region, all regions show earlier simulated dates from budburst to grape theoretical maturity when comparing the 1992–2021 to 1962–1991 periods. For all stages, the shift is strongest for OCE regions. Changes in budburst range from –4 days (Grenache in Bouches-du-Rhône and Provence) to –12 days (Pinot noir in Beaujolais). Simulated shifts in the mid-flowering range from –6 days (Grenache in Bouches-du-Rhône, Provence and Pyrénées-Orientales) to 14 days (Pinot noir in Beaujolais). Changes in earliness of mid-veraison are also strongest in Beaujolais (21 days) and smallest in Provence and Pyrénées-Orientales.

Looking at grape varieties, Chardonnay (Champagne) shows the highest advance in simulated maturity (21 days) on average in the 1992–2021 period compared to 1960–1991. The shift in theoretical maturity of Riesling (Alsace) and Syrah (Côtes-du-rhône Nord) came in 2nd and 3rd place with an advance in 17 and 16 days earlier, respectively, in 1992-2021. Pinot noir (Bourgogne, Beaujolais, Jura, Bugey-Savoie, Cher), Cabernet franc (Val de Loire) and Cabernet-Sauvignon (Bordelais, Dordogne, Lot-et-Garonne, Cahors, Gers, Gaillac) have on average a similar advance ranging from 13.5 to 15 days. Ugni blanc (Charentes) and Grenache (MED regions) have the lowest advance in phenology stages simulated and show an earlier modelled maturity of 11 and 12 days, respectively.

This increased earliness observed on all phenological stages, including maturity is not equal and is increasing over the growing season, leading to a shorter budburst-maturity period. This compression is observed in almost all wine regions ranging from 4.4 to 9.5 days (see supplementary data Table S1) and takes place mainly during the flowering-maturity period (no significant change during the budburst-flowering period; i.e., supplementary data Table S1).

TABLE 3. Mean evolution of agroclimatic indices projected over the 2041–2070 period with 19 CMIP6 models according to SSP2-4.5 and SSP5-8.5. Values correspond to the median of the 19 models' mean differences between the 1985–2014 and 2041–2070 periods averaged over wine regions. Values with * indicate a significant difference between the two periods for at least half of the 19 models. The standard deviation of the 19 models is indicated after the ± symbol.

Climate influence	Cultivar	Wine-growing Regions	mGST [°C]		mGSP [mm]	
			SSP2-4.5	SSP5-8.5	SSP2-4.5	SSP5-8.5
Semi-Continental and Oceanic	Riesling	Alsace	1.9 ± 0.6 *	2.4 ± 0.8 *	5 ± 33	-21 ± 33
	Chardonnay	Champagne	1.7 ± 0.6 *	2.3 ± 0.9 *	0 ± 25	-26 ± 32
	Pinot noir	Bourgogne	1.9 ± 0.6 *	2.5 ± 0.9 *	-4 ± 31	-38 ± 31
		Beaujolais	2 ± 0.6 *	2.7 ± 0.9 *	-7 ± 35	-34 ± 35
		Jura	1.9 ± 0.6 *	2.6 ± 0.9 *	-5 ± 48	-51 ± 49
		Bugey-Savoie	1.9 ± 0.6 *	2.7 ± 0.8 *	-24 ± 45	-75 ± 52
		Cher	1.7 ± 0.6 *	2.4 ± 0.9 *	-14 ± 23	-40 ± 28
Oceanic	Cabernet franc	Val de Loire	1.6 ± 0.6 *	2.2 ± 0.9 *	-23 ± 19	-42 ± 29 *
	Ugni blanc	Charentes	1.7 ± 0.6 *	2.4 ± 0.8 *	-23 ± 23	-58 ± 28 *
	Cabernet-Sauvignon	Bordelais	1.8 ± 0.6 *	2.4 ± 0.8 *	-26 ± 28	-60 ± 31 *
		Dordogne	1.8 ± 0.6 *	2.4 ± 0.8 *	-31 ± 31	-63 ± 34 *
		Lot-et-Garonne	1.8 ± 0.6 *	2.4 ± 0.7 *	-30 ± 34	-69 ± 36 *
		Cahors	1.9 ± 0.6 *	2.7 ± 0.8 *	-33 ± 33	-74 ± 41 *
		Gers	1.8 ± 0.6 *	2.5 ± 0.8 *	-33 ± 34	-72 ± 38 *
		Gaillac	2 ± 0.6 *	2.8 ± 0.8 *	-33 ± 31	-53 ± 35 *
Mediterranean	Syrah	Côtes-du-rhône Nord	2.1 ± 0.5 *	2.9 ± 0.8 *	-12 ± 40	-40 ± 40
	Grenache	Côtes-du-rhône Sud	2.1 ± 0.6 *	3.1 ± 0.8 *	-39 ± 39	-60 ± 40
		Bouches-du-Rhône	2.3 ± 0.5 *	3.3 ± 0.7 *	-32 ± 36	-47 ± 33
		Provence	2.3 ± 0.5 *	3.6 ± 0.7 *	-40 ± 40	-52 ± 41
		Languedoc	2 ± 0.5 *	2.9 ± 0.7 *	-27 ± 33	-51 ± 37
		Pyrénées-Orientales	2.1 ± 0.5 *	2.8 ± 0.8 *	-24 ± 34	-47 ± 40
All regions average			1.9 ± 0.5 *	2.7 ± 0.8 *	-27 ± 26	-49 ± 29

mGST = April-to-Sept. average temperature; mGSP = April-to-Sept. precipitation

Higher temperatures projected in the mid-21st century have a direct impact on simulated phenological stages obtained with cumulative degree days models. Hence, the simulated advance of all the phenological phases in the past (SAFRAN) is clearly accentuated for the 2041–2070 period (Table 4). Wine regions under SCO influence (where Riesling, Chardonnay and Pinot noir are cultivated) show the highest increased earliness for veraison (15 to 19 days average according to SSP2 and SSP5) and theoretical maturity (20 to 27 days average according to SSP2 and SSP5). OCE and MED regions have a simulated advance for veraison of 13 and 16 days (SSP2) on average and 17 to 21 days (SSP5) on average (Table 4).

Budburst is the phenological stage simulated with the highest variability between grape varieties. It could be earlier by 3 to 13 days (SSP2) and 3 to 18 days (SSP5). Wine regions such as Val de Loire (13 to 18 days according to SSP) or Cahors (11 to 14 days) present the earliest projected budburst while all MED regions (with Grenache) present the lowest advance (between 3 to 7 days according to SSP). For Grenache, a particular trend is observed in the MED region: shift towards an earlier budburst is slightly smaller with SSP5 than for SSP2, even though the latter lead to a lower rise in temperature than the first. In Pyrénées-Orientales, the change in budburst dates in the 2050s, compared to 1985–2014, is not significant with SSP5, while it is with SSP2. Higher winter temperatures may negatively impact the accumulation of cold units needed to break dormancy, hence delaying budbreak for this grape variety in these wine regions.

In contrast to budburst, flowering is the phenological stage for which variability related to the grape variety or the wine region is lowest. It is projected to be earlier on average by 8 to 11 days according to the SSP pathway considered.

The strongest change is observed for modelled maturity dates. In 2041–2070 it is anticipated to be 30 days earlier in Champagne, in comparison to 2041–2070. The projected change in modelled maturity is lower in OCE and MED regions (from –15 to –25 days, according to the region/cultivar/SSP).

Shift in modelled maturity is 1 to 10 days higher than the shift in mid-veraison date, suggesting a shorter ripening period in all regions. The results presented here suggest that veraison-to-harvest duration would range from 20 days (Chardonnay for Champagne wine, SSP5) to 38 days (Riesling at 190 g/L in Alsace, SSP2).

3. Ecoclimatic indices

The median number of frost days after budburst (FrostDays) does not change significantly in all wine regions for both past periods (Table 2) and projected future periods (Table 5). It slightly decreases when considering the mean value of CMIP6 models (results not shown).

As for FrostDays, the three ecoclimatic indices FRD.BB.FLO15, CR.BB.FLO15 (respectively frequency of rainy days and cumulative precipitations from budburst to 15 days after flowering) and SRD.5FLO5 (number of rainy days 5 days before to 15 days after flowering) do not show any significant evolution in all wine regions for both past periods (Table 2) and projected future period (Table 5). The large variance between climate models suggests that change in precipitation during spring and the flowering period is highly uncertain so it is not possible to conclude about the impact of precipitation change on the number of days suitable for mechanical work in vineyards, diseases risk and conditions for pollination and fruit set. However, as seen previously with the agroclimatic index mGSP, the cumulative rainfall from April to September tends to decrease. This decrease is significant in OCE wine regions with SSP5. Regarding the simulated budburst-maturity period, this decrease in accumulated rainfall could be much stronger and more significant in all wine regions (see supplementary data Table S2). When a maturity date fixed at 35 days after mid-veraison is used, the decrease is slightly attenuated in some regions. Hence, the decrease in rainfall during the growing season will, most likely, take place between fruit set and harvest.

Decreased rainfall combined with increased temperatures projected by SSP2 and SSP5 for the mid-21st century would lead to increased water stress (HydricSI; Table 5) between flowering and maturity. This increase is significant in 5 out of 21 situations for SSP2 and in 14 out of 21 situations for SSP5. OCE regions show the largest increase while the SCO regions do not show a significant change with SSP2 (except for Pinot noir in Bugey–Savoie), but would all be significantly impacted with SSP5 (except for Riesling in Alsace). The MED regions have all decreasing mean HydricSI values, but the trend is not significant (except for Syrah in Côtes-du-rhône Nord) regardless of the SSP considered. This can be explained by the high GCM inter-model variability and the compression of the VER-MAT period. Indeed, considering a fixed length of the VER-MAT period (35 days), the water stress increase (decrease of HydricSI values) and for some regions (Côtes-du-rhône Sud, Languedoc and Pyrénnées-Orientales), the trend would be significant (see supplementary data Table S3). Considering the past evolution (1962–1991 vs 1992–2021 with SAFRAN data), no significant change in the HydricSI index is observed on average, except for the Bouches-du-Rhône wine region (Table 2).

With higher temperatures during the flowering period, projected thermal conditions (as expressed by the Wang and Engel index mean value WE.5FLO15) are more favourable to photosynthesis activity. This index increased in all wine regions with a significant evolution for 12 of 21 wine regions (Table 2). As projected hydric stress during this period remains very low (< 0.05 on average, i.e., no stress, results not shown) for the middle of the 21st century, climate conditions during flowering are expected to be in favour of increased fruit set, and, possibly yield.

Finally, looking at the number of heat days (with Tmax > 35 °C) a significant increase during the past period is only observed in three wine regions (Cahors, Gaillac, and Côtes-du-rhône Sud). This is clearly due to the high number of years with the HeatDays index equal to zero during the 1962–2021 period.

TABLE 4. Mean evolution of phenological stages projected over the 2041–2070 period with 19 CMIP6 models according to SSP2-4.5 and SSP5-8.5 emission scenarios. Values correspond to the median of the 19 models' mean differences between the 1985–2014 and 2041–2070 periods averaged over wine regions. Values with * indicate a significant difference between the two periods for at least half of the 19 models. The standard deviation of the 19 models is indicated after the ± symbol.

Climate influence	Cultivar	Wine-growing Regions	BUD [doy]		FLO [doy]		VER [doy]		MAT [doy]	
			SSP2-4.5	SSP5-8.5	SSP2-4.5	SSP5-8.5	SSP2-4.5	SSP5-8.5	SSP2-4.5	SSP5-8.5
Semi-Continental and Oceanic	Riesling	Alsace	-10 ± 3 *	-13 ± 4 *	-9 ± 3 *	-10 ± 3 *	-16 ± 4 *	-20 ± 5 *	-23 ± 6 *	-30 ± 7 *
	Chardonnay	Champagne	-8 ± 3 *	-11 ± 4 *	-8 ± 3 *	-10 ± 4 *	-15 ± 4 *	-20 ± 5 *	-18 ± 5 *	-25 ± 6 *
	Pinot noir	Bourgogne	-8 ± 3 *	-10 ± 3 *	-8 ± 3 *	-10 ± 3 *	-14 ± 4 *	-18 ± 4 *	-20 ± 5 *	-25 ± 6 *
		Beaujolais	-8 ± 3 *	-10 ± 3 *	-9 ± 3 *	-11 ± 3 *	-15 ± 4 *	-18 ± 4 *	-21 ± 5 *	-26 ± 6 *
		Jura	-9 ± 3 *	-11 ± 3 *	-9 ± 3 *	-11 ± 3 *	-15 ± 4 *	-19 ± 5 *	-21 ± 5 *	-26 ± 6 *
		Bugey-Savoie	-9 ± 3 *	-13 ± 3 *	-10 ± 2 *	-12 ± 3 *	-16 ± 4 *	-22 ± 4 *	-21 ± 6 *	-29 ± 6 *
		Cher	-7 ± 3 *	-10 ± 3 *	-8 ± 3 *	-10 ± 3 *	-14 ± 4 *	-17 ± 5 *	-18 ± 5 *	-24 ± 6 *
Oceanic	Cabernet franc	Val de Loire	-13 ± 4 *	-18 ± 5 *	-7 ± 2 *	-10 ± 3 *	-13 ± 4 *	-17 ± 5 *	-16 ± 5 *	-22 ± 6 *
	Ugni blanc	Charentes	-6 ± 2 *	-9 ± 3 *	-7 ± 2 *	-9 ± 3 *	-13 ± 4 *	-16 ± 4 *	-17 ± 4 *	-22 ± 5 *
	Cabernet-Sauvignon	Bordelais	-9 ± 3 *	-12 ± 4 *	-7 ± 2 *	-9 ± 3 *	-12 ± 3 *	-14 ± 4 *	-15 ± 4 *	-19 ± 5 *
		Dordogne	-10 ± 3 *	-13 ± 4 *	-7 ± 2 *	-10 ± 3 *	-12 ± 3 *	-15 ± 4 *	-16 ± 4 *	-20 ± 5 *
		Lot-et-Garonne	-10 ± 3 *	-13 ± 4 *	-7 ± 2 *	-10 ± 3 *	-12 ± 3 *	-15 ± 4 *	-15 ± 4 *	-20 ± 5 *
		Cahors	-11 ± 3 *	-14 ± 4 *	-8 ± 2 *	-11 ± 3 *	-13 ± 3 *	-16 ± 4 *	-18 ± 4 *	-22 ± 4 *
		Gers	-10 ± 3 *	-13 ± 4 *	-7 ± 2 *	-10 ± 3 *	-12 ± 3 *	-15 ± 4 *	-16 ± 4 *	-21 ± 5 *
		Gaillac	-10 ± 3 *	-13 ± 4 *	-8 ± 2 *	-11 ± 3 *	-13 ± 3 *	-16 ± 4 *	-16 ± 4 *	-21 ± 4 *
Mediterranean	Syrah	Côtes-du-rhône Nord	-9 ± 2 *	-11 ± 3 *	-9 ± 2 *	-12 ± 3 *	-15 ± 3 *	-19 ± 4 *	-19 ± 4 *	-25 ± 5 *
	Grenache	Côtes-du-rhône Sud	-6 ± 2 *	-7 ± 3 *	-9 ± 3 *	-12 ± 3 *	-15 ± 3 *	-18 ± 4 *	-16 ± 4 *	-22 ± 4 *
		Bouches-du-Rhône	-6 ± 2 *	-5 ± 2 *	-9 ± 2 *	-12 ± 3 *	-14 ± 3 *	-18 ± 3 *	-16 ± 3 *	-21 ± 3 *
		Provence	-6 ± 2 *	-5 ± 2 *	-10 ± 3 *	-13 ± 4 *	-14 ± 3 *	-19 ± 4 *	-16 ± 3 *	-22 ± 3 *
		Languedoc	-4 ± 2 *	-4 ± 2 *	-8 ± 2 *	-11 ± 3 *	-12 ± 3 *	-16 ± 3 *	-15 ± 3 *	-19 ± 3 *
		Pyrénées-Orientales	-3 ± 1 *	-3 ± 2	-7 ± 2 *	-10 ± 3 *	-12 ± 3 *	-15 ± 4 *	-15 ± 3 *	-19 ± 4 *
All regions average			-7 ± 2 *	-10 ± 3 *	-8 ± 2 *	-11 ± 3	-13 ± 3 *	-17 ± 4 *	-16 ± 4	-22 ± 4 *

BUD = budburst; FLO = mid-flowering; VER = veraison; MAT = theoretical maturity.

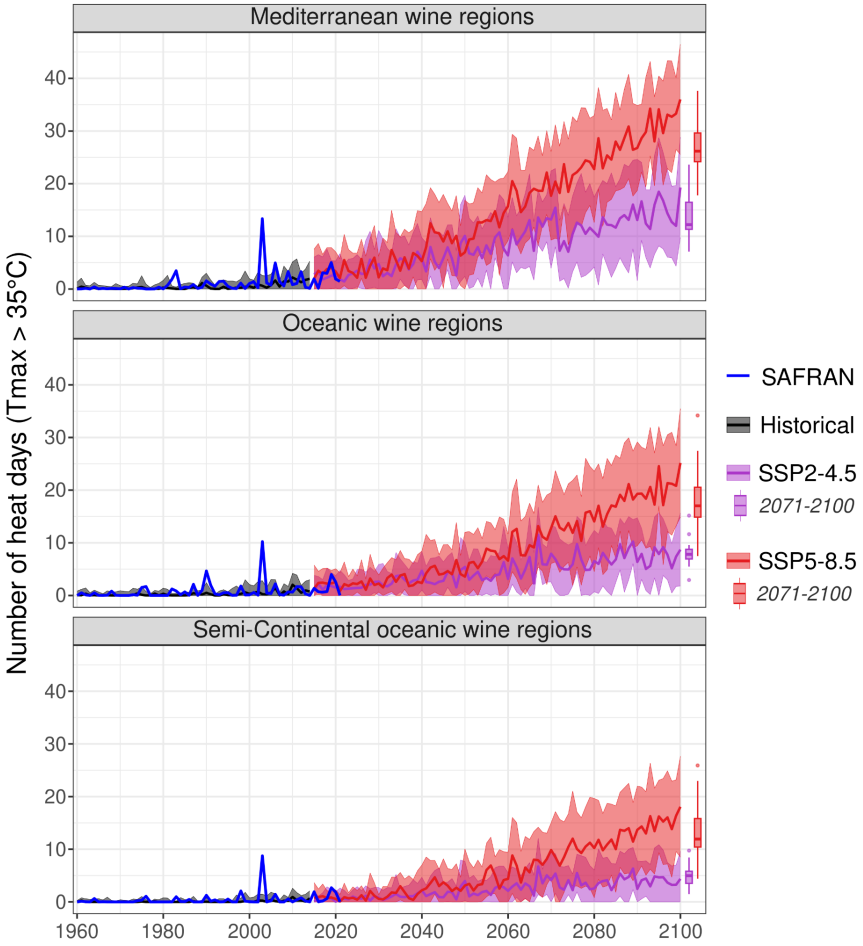

FIGURE 3. Evolution of HeatDays between budburst and simulated theoretical maturity averaged over French wine regions (Figure 1). Calculations are based on SAFRAN data (1960–2022) and simulated with 19 CMIP6 models according to SSP2-4.5 and SSP5-8.5 emission scenarios. The curve representing the evolution of the index obtained from GCM data corresponds to the median of all models tested with standard deviation (ribbon). Boxplots are made with the index average for each GCM model over the 2071–2100 period.

However, looking at the trend evolution during this period, all regions show a significant increase (Figure 3). The year 2003 was marked by a heatwave affecting all of Western Europe. Respectively, 13 HeatDays (MED regions), 10 HeatDays (OCE regions) and 8 HeatDays (SCO regions; Figure 3) were recorded on average. During this year, some wine regions like Cahors or Gaillac recorded an average of 18 days of HeatDays.

Using projected climate data, the number of heat days will substantially increase in all wine regions (Table 5 and Figure 3) and the trend is significant for most regions. The regions under MED influence would be affected by the greatest increase with +9 to +15 days (for, respectively, SSP2 and SSP5) followed by OCE regions with +8 to +13 days and SCO regions with +4 to +7 days simulated during the 2041-2070 period. By the end of the 21st century (Figure 3), the number of HeatDays could dramatically increase to reach an average between +12 to +26 days (MED regions, according to the SSP pathway considered) to +5 to +12 days (SCO regions). 2003 would then be considered a typically "cold" or even "very cold" year according to SSP5 projections (considering heat days) and a "normal" year according to SSP2 projections.

Maintaining a fixed duration of 35 days between veraison and harvest is sometimes considered in studies based on ecoclimatic indicators (Bécart *et al*., 2022). This approach allows us to observe the expected increase in grape sugar content, based on the linear interpolation (and extrapolation up to 250 $g.L^{-1}$) between cumulative degree days and sugar content from the values provided by Parker *et al*. (2020) (Figure 4). Our approach simulates a very short ripening window in Champagne for the current period (24 days on average, Figure 4). A very short ripening window is simulated as well for Grenache, with a sugar threshold set at 210 $g.L^{-1}$. Riesling is the grape variety with the longest simulated VER-MAT period (48 days over the historical period). This period could be reduced by 10 to 12 days according to SSP2 and SSP5 respectively. Ugni blanc, Pinot noir, Cabernet-Sauvignon, Cabernet franc and Syrah have a simulated ripening window between 34 and 37 days over the historical period, which could be reduced by 4 to 5 days with SSP2 and 6 to 7 days with SSP5 by the middle of the 21st century.

TABLE 5. Mean evolution of ecoclimatic indices projected over the 2041–2070 period with 19 CMIP6 models according to SSP2-4.5 and SSP5-8.5. Values correspond to the median of the 19 models' mean differences between the 1985–2014 and 2041–2070 periods averaged over wine regions. Values with * indicate the presence of a significant difference between the two periods for at least half of the 19 models. The standard deviation of the 19 models is indicated after the ± symbol.

Climate influence	Cultivar	Wine-growing Regions	FrostDays [days]		HeatDays [days]		FRD.BB.FLO15 [%]		CR.BB.FLO15 [mm]		SRD.5FLO15 [days]		WE.5FLO15 [unitless]		HydricSI [unitless]	
			SSP2-4.5	SSP5-8.5	SSP2-4.5	SSP5-8.5	SSP2-4.5	SSP5-8.5	SSP2-4.5	SSP5-8.5	SSP2-4.5	SSP5-8.5	SSP2-4.5	SSP5-8.5	SSP2-4.5	SSP5-8.5
Semi-Continental and Oceanic	Riesling	Alsace	-0.4 ± 0.2	-0.4 ± 0.2	2 ± 1	4 ± 3	-1.2 ± 2.1	-2.5 ± 2.8	10 ± 17	5 ± 25	-0.3 ± 0.9	-0.9 ± 0.9	0.044 ± 0.022	0.067 ± 0.024 *	-0.047 ± 0.033	-0.061 ± 0.044
	Chardonnay	Champagne	-0.1 ± 0.4	-0.2 ± 0.3	2 ± 1 *	3 ± 3 *	-0.9 ± 2.3	-2 ± 2.4	3 ± 14	-2 ± 19	-0.4 ± 0.9	-0.6 ± 0.9	0.041 ± 0.022	0.06 ± 0.024 *	-0.055 ± 0.041	-0.099 ± 0.055 *
	Pinot noir	Bourgogne	-0.1 ± 0.2	-0.1 ± 0.2	3 ± 2 *	6 ± 4 *	-0.7 ± 2.1	-2.3 ± 2.6	7 ± 16	-4 ± 19	0.1 ± 0.9	-0.4 ± 0.8	0.032 ± 0.021	0.063 ± 0.024 *	-0.062 ± 0.038	-0.105 ± 0.041 *
		Beaujolais	-0.1 ± 0.2	-0.1 ± 0.2	4 ± 2 *	7 ± 4 *	-0.4 ± 2.5	-2.7 ± 2.6	5 ± 19	-6 ± 21	0.3 ± 1	-0.6 ± 0.9	0.034 ± 0.023	0.066 ± 0.026 *	-0.048 ± 0.035	-0.075 ± 0.036 *
		Jura	-0.2 ± 0.2	-0.2 ± 0.1	2 ± 2 *	5 ± 3 *	-0.4 ± 2.3	-2 ± 2.8	18 ± 24	2 ± 31	0.1 ± 1	-0.4 ± 1	0.038 ± 0.022	0.06 ± 0.026 *	-0.04 ± 0.024	-0.068 ± 0.034 *
		Bugey-Savoie	-0.4 ± 0.2	-0.3 ± 0.2	2 ± 1	4 ± 4	-1.2 ± 2.9	-3.4 ± 2.9	5 ± 26	-16 ± 28	0.1 ± 1.1	-0.4 ± 1	0.045 ± 0.024 *	0.066 ± 0.025 *	-0.048 ± 0.024 *	-0.072 ± 0.035 *
		Cher	-0.2 ± 0.3	-0.4 ± 0.2	3 ± 2 *	5 ± 4 *	-1.8 ± 1.9	-2.1 ± 2.2	0 ± 13	-7 ± 15	-0.1 ± 0.9	-0.6 ± 0.8	0.033 ± 0.022	0.055 ± 0.024 *	-0.06 ± 0.043	-0.103 ± 0.051 *
Oceanic	Cabernet franc	Val de Loire	0 ± 0.3	-0.1 ± 0.3	2 ± 2 *	4 ± 3 *	-1 ± 1.7	-1.5 ± 1.7	8 ± 14	9 ± 15	0.2 ± 1	-0.2 ± 0.8	0.032 ± 0.022	0.051 ± 0.023 *	-0.061 ± 0.044	-0.109 ± 0.051 *
	Ugni blanc	Charentes	0 ± 0.1	0 ± 0	4 ± 2 *	6 ± 3 *	-1.3 ± 2	-2.7 ± 2.3	-3 ± 15	-14 ± 18	-0.1 ± 1	-0.5 ± 0.8	0.039 ± 0.02	0.047 ± 0.023 *	-0.066 ± 0.044 *	-0.118 ± 0.049 *
	Cabernet-Sauvignon	Bordelais	-0.1 ± 0.2	-0.2 ± 0.2	4 ± 2 *	7 ± 4 *	-1 ± 2	-3.2 ± 2	0 ± 18	-10 ± 18	0 ± 1	-0.7 ± 0.8	0.034 ± 0.019	0.046 ± 0.021 *	-0.066 ± 0.044	-0.112 ± 0.05 *
		Dordogne	0 ± 0.3	-0.1 ± 0.2	5 ± 2 *	8 ± 3 *	-0.8 ± 2.1	-3.4 ± 2.2	3 ± 20	-13 ± 21	0 ± 1.1	-0.9 ± 0.8	0.029 ± 0.018	0.044 ± 0.02 *	-0.061 ± 0.048	-0.108 ± 0.052 *
		Lot-et-Garonne	0 ± 0.3	-0.1 ± 0.2	5 ± 3 *	8 ± 4 *	-1.1 ± 2.1	-3.7 ± 2.2	0 ± 20	-10 ± 19	0 ± 1.1	-0.9 ± 0.8	0.03 ± 0.019	0.044 ± 0.02 *	-0.069 ± 0.048 *	-0.101 ± 0.051 *
		Cahors	0 ± 0.3	0 ± 0.2	7 ± 4 *	13 ± 5 *	-1.2 ± 2.1	-3.2 ± 2.3	8 ± 21	-17 ± 23	-0.2 ± 1	-0.5 ± 0.8	0.036 ± 0.022	0.053 ± 0.025 *	-0.075 ± 0.051 *	-0.114 ± 0.055 *
		Gers	0 ± 0.3	-0.2 ± 0.2	6 ± 4 *	9 ± 5 *	-1.4 ± 2	-4.3 ± 2.4	1 ± 23	-14 ± 21	-0.1 ± 1.1	-0.6 ± 0.8	0.031 ± 0.02	0.046 ± 0.02 *	-0.073 ± 0.044 *	-0.117 ± 0.049 *
		Gaillac	0 ± 0.2	-0.1 ± 0.2	8 ± 4 *	12 ± 5 *	-1.4 ± 2.4	-4.2 ± 2.5	-4 ± 19	-19 ± 18	-0.3 ± 1.1	-0.7 ± 0.8	0.035 ± 0.02	0.054 ± 0.023 *	-0.063 ± 0.045	-0.067 ± 0.051
Mediterranean	Syrah	Côtes-du-rhône Nord	-0.2 ± 0.2	-0.2 ± 0.1	6 ± 2 *	11 ± 4 *	-0.5 ± 2.3	-2.7 ± 2.5	3 ± 19	-7 ± 23	0.4 ± 0.9	-0.4 ± 0.8	0.036 ± 0.021	0.06 ± 0.024 *	-0.063 ± 0.036	-0.099 ± 0.04 *
	Grenache	Côtes-du-rhône Sud	-0.1 ± 0.1	-0.2 ± 0.1	9 ± 3 *	14 ± 4 *	-0.8 ± 1.9	-2.6 ± 1.8	-6 ± 21	-22 ± 20	-0.2 ± 0.9	-0.5 ± 0.6	0.039 ± 0.017 *	0.056 ± 0.018 *	-0.036 ± 0.036	-0.051 ± 0.041
		Bouches-du-Rhône	0 ± 0	0 ± 0	7 ± 2 *	12 ± 4 *	-0.6 ± 1.8	-2.7 ± 1.7	-8 ± 20	-20 ± 16	-0.1 ± 0.6	-0.5 ± 0.4	0.04 ± 0.019 *	0.058 ± 0.017 *	-0.024 ± 0.029	-0.022 ± 0.038
		Provence	0 ± 0.1	0 ± 0.1	9 ± 3 *	15 ± 4 *	-0.9 ± 2.2	-3.2 ± 2	-13 ± 24	-35 ± 20	-0.2 ± 0.7	-0.5 ± 0.4	0.041 ± 0.02 *	0.06 ± 0.017 *	-0.022 ± 0.033	-0.022 ± 0.04
		Languedoc	0 ± 0	0 ± 0	7 ± 3 *	12 ± 4 *	-1.7 ± 1.8	-3.4 ± 2	-11 ± 18	-22 ± 19	-0.3 ± 0.7	-0.6 ± 0.6	0.036 ± 0.014 *	0.052 ± 0.017 *	-0.034 ± 0.03	-0.052 ± 0.042
		Pyrénées-Orientales	0 ± 0	0 ± 0	5 ± 2 *	9 ± 4 *	-1.7 ± 1.7	-3.7 ± 2.2	-13 ± 19	-25 ± 24	-0.1 ± 0.7	-0.5 ± 0.7	0.036 ± 0.016	0.05 ± 0.019 *	-0.028 ± 0.033	-0.042 ± 0.049
All regions average			-0.1 ± 0.1	-0.1 ± 0.1	5.3 ± 2.1 *	8.7 ± 3.4 *	-1.4 ± 1.6	-3.2 ± 1.8	-2 ± 12	-14 ± 14	-0.1 ± 0.7	-0.6 ± 0.6	0.035 ± 0.015	0.054 ± 0.019 *	-0.051 ± 0.032	-0.092 ± 0.038 *

FrostDays = count of days with min. temperature below 0 °C between BUD and MAT; HeatDays: count of days with max. temperature over 35 °C between BUD and MAT; FRD.BB.FLO15 = frequency of days with precipitation from BUD to 15 days after FLO; CR.BB.FLO15 = precipitation from BUD to 15 days after FLO; SRD.5FLO15 = count of days with precipitation 5 days before to 15 days after FLO; WE.5FLO15 = average heat units calculated daily with the Wang-and-Engel function, 5 days before to 15 days after FLO; HydricSI = stress index corresponds to 1 - average of daily relative stomatal conductance of grapevine between flowering and maturity.

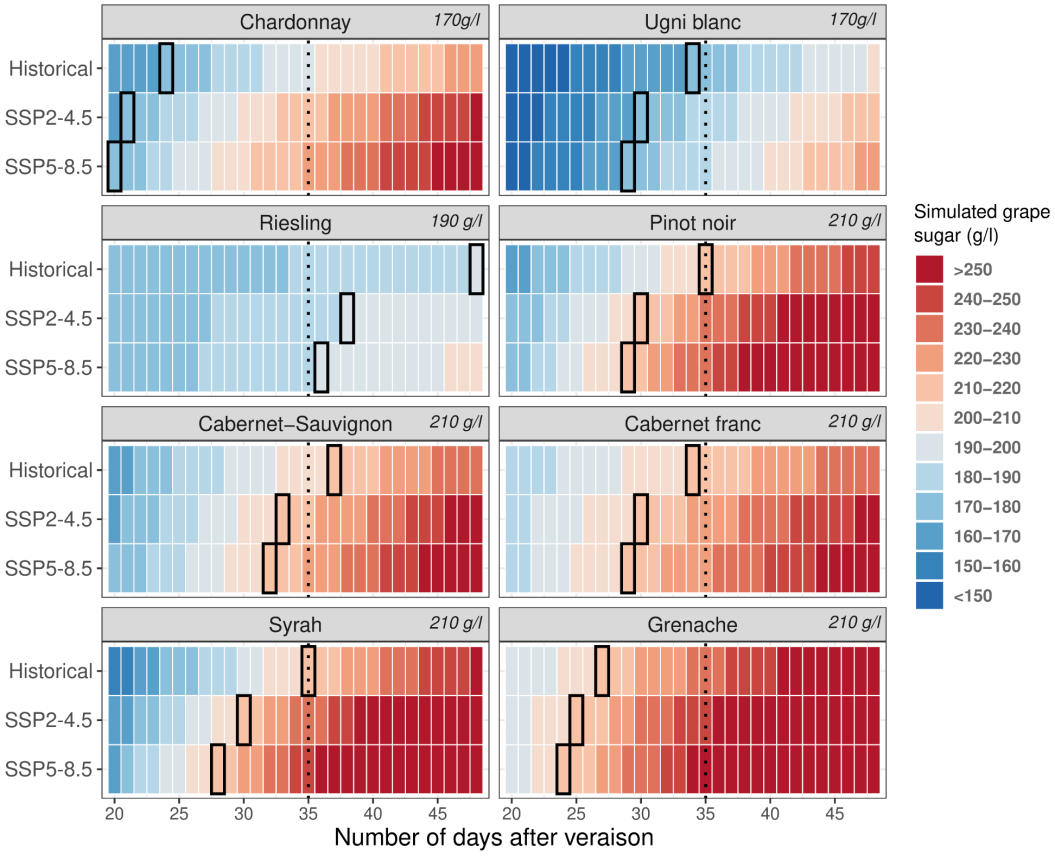

FIGURE 4. Evolution of sugar content in grapes simulated with GSR for a 20 to 48 days window after mid-veraison. Calculations are made using the average simulated sugar content value of grid cells of wine regions related to each cultivar (see Figure 1). For projected climate data the median of the 19 GCM is used. Each box represents the day from which the simulated grape sugar concentration (written in the box next to the grape variety) is reached.

DISCUSSION

1. A spatial scale possibly underestimating extremes

The SAFRAN database, with an 8 km resolution, enables the selection of a set of grid cells whose spatial representativeness is intrinsically homogeneous and proportional to the wine-growing region's surfaces. In addition, a significant time depth is available (since 1959) with no missing data. However, there are some limitations to the use of the SAFRAN database. The comparison over the recent period between SAFRAN and weather station data in Burgundy and Champagne shows some bias with similar seasonal characteristics on minimum and maximum temperatures (Zito, 2021). These biases occur particularly during spring and summer, with minimum temperature overestimated (0.8 to 1 °C) and maximum temperatures underestimated (1 to 1.4 °C). Other studies comparing SAFRAN to observed climate data find similar biases in France (Vidal *et al*., 2010). Hence, the use of SAFRAN data leads to an underestimation of thermal extremes compared to weather station records, and, particularly in a wine-growing area. Vineyards are often established on rugged topography areas, enhancing local climate diversity as previously observed in France (Bois, 2007; Bonnefoy, 2013; Cuccia, 2013; de Rességuier *et al*., 2020).

Ecoclimatic indices using a threshold temperature such as FrostDays and HeatDays may potentially be underestimated in magnitude, depending on the wine region. Concerning spring frost risk, in addition to the potential overestimation of minimum temperatures, projections for viticulture in Europe throughout the 21st century (Sgubin *et al*., 2018) show that its evolution strongly depends on the model chosen to simulate budburst. A recent study (Gavrilescu *et al*., 2022) compared six spring frost models with budburst simulation on Chardonnay in Burgundy with projected climate evolution throughout the 21st century. Three models show a decrease in the frequency of frost years across the whole study area while the two others show an increase that is more or less pronounced depending on the regions.

Hence, despite the large number of GCMs and their resolution used to study the future evolution of spring frost risk with climate change, the lack of precision in grapevine budburst and dehardening models makes projections of spring frost risk particularly uncertain.

2. Changes in phenology

Simple and commonly used phenological models were applied to calculate different key phenological stages and ecoclimatic indices at a regional scale. Here, models were not directly validated with observed local data. However, other studies have already validated their use at a

regional scale with observed phenology data: Bécart *et al*. (2022) for Grenache in Côtes-du-rhône Sud wine region, Zito (2021) for Pinot noir and Chardonnay in Champagne and Burgundy.

The global phenology trends simulated over French wine-growing regions confirm results obtained in previous studies in other vineyards around the world (see Droulia and Charalampopoulos, 2021 review). All phenological stages are affected by warmer conditions and will take place more or less earlier, depending on the SSP emission scenario, cultivar and wine region. The greater earliness simulated in SCO regions confirms the conclusion of previous studies such as García de Cortázar-Atauri *et al*. (2017) observing earlier phenological stages in northern than in southern French vineyards (using three cultivars and CMIP5 climate data). Droulia and Charalampopoulos (2021) note that the general earlier occurrence of phenological stages follows a latitudinal and longitudinal geographical gradient over Europe, with earlier projected budbreak and flowering over north-eastern Europe and smaller changes over western/southern Europe.

Regarding budburst simulation, the use of models integrating chilling forcing one to simulate dormancy release, such as SUWE or the BRIN model from García de Cortázar-Atauri *et al*. (2009), revealed to be important in the context of climate change. The delay of an endo-dormancy break because of insufficient chilling may offset the advance caused by higher temperature during the eco-dormancy phase, or even cause a delay in the budburst date (Caffarra and Eccel, 2010; Chuine *et al*., 2016; Webb *et al*., 2007).

Moreover, for stages from flowering to maturity, GFV and GSR models do not consider the potential effect of excessively high temperatures during summer that could slow down grapevine growth and development, leading to an increased duration of phenological phases. Indeed, Molitor *et al*. (2014) and Molitor *et al*. (2020), demonstrate that using an upper threshold temperature above which a further increase in temperature will not accelerate plant development and a heat threshold, above which a further increase in the temperature leads to a development deceleration, could significantly improve model accuracy compared to cumulative degree day approaches.

3. Harvest and modelled maturity simulated with grape sugar threshold

The prediction of harvest dates based on grape sugar concentration simulated with models based only on temperature is not always relevant. Despite the very strong link between temperature and harvest dates, which has been used as accurate proxies to study past climate evolutions (Daux *et al*., 2012; Labbé *et al*., 2019; Chuine *et al*., 2004), many other factors contribute to the timing of harvest. Among these factors, bunch rot or vine water status (Webb *et al*., 2012), air CO_2 concentration (Martínez-Lüscher *et al*., 2016) or simply the style of wine desired by the winegrower (van Leeuwen and Destrac-Irvine, 2017). Moreover, grapes are sometimes harvested before the desired sugar concentration, because the ripening window closes at the end of October in the northern hemisphere.

In several studies, the harvest date is set to a fixed number of days after veraison, generally 35 or 40. This approach is relevant in many cases, but probably generates inconsistencies in future projections, especially for regions such as Champagne where a fixed duration would certainly lead to harvesting grapes at too high sugar and too low acidity for the production of sparkling wines. Moreover, the day of harvest does not only depend on the timing of mid-veraison but also on grape ripening dynamics, which are likely to be impacted by temperature.

In the MED regions, despite warmer conditions, there is a tendency to maintain a longer time between veraison and harvest, leading to an increase in the sugar content of the grapes at maturity, as reported by Bécart et al. (2022). These authors indicate that in the southern Rhône valley, Grenache is harvested at about 14 % vol. alcohol (i.e., the sugar content of 23.8 °Brix, 235 $g.L^{-1}$). Hence, our simulated harvest dates are earlier than real harvest dates. This issue does not have a major impact on the conclusions, as we focus mainly on trends in harvest dates across time periods, climate change scenarios, varieties and regions, and not on absolute harvest dates.

In the case of Champagne, the underestimation of the veraison/harvest duration may be related to specific leaf/fruit ratios in that region. With a high fruit load to achieve high yields in Champagne, low leaf area/fruit weight ratios may slow down sugar accumulation in bunches and berries (Morinaga *et al*., 2000).

Conversely, our simulations show that Riesling is harvested on average 48 days after veraison (Figure 4). This duration is probably over-estimated by not taking into account the particular topographical position (steep slopes) of the Alsace vineyards, exposed to the east, offering more favourable topo-climatic conditions than those provided by gridded SAFRAN data. In other cases, growers take advantage of warmer conditions to pick fruit at greater levels of ripeness such as in Saint-Emilion vineyards near Bordeaux, where the observed duration veraison-harvest from 1988 to 2014 has been increasing from 40 to 65 days for Cabernet franc (van Leeuwen and Darriet, 2016).

Allowing a long duration between mid veraison and harvest (so-called "hang time") is sometimes desired to ensure good ripening of the grapes, for which growers take into account technological maturity (sugar/acidity/pH), phenolic maturity (Rajha et al., 2017) and aromatic maturity (van Leeuwen et al., 2022). Maintaining a long "hang time" would result in the harvest of grapes with average sugar levels probably above 250 g.L-1(25 °Brix, 15 % vol. potential alcohol) by 2050 for Grenache in south-eastern France (under the SSP5 emission scenario). In Alsace, Riesling is expected to reach almost 210 g.L-1 (Figure 4). These values can be modulated by viticultural practices to slow down grape ripening (Palliotti et al., 2014).

It should be noted that a longer period between veraison and harvest will expose grapevines to higher water deficit stress (see simulated HydricSI in the 35-day fixed veraison-harvest period, supplementary data Table S3).

CONCLUSION

Projecting changes in vineyards for the future is a highly uncertain exercise, as many factors may affect grapevine growth, cropping conditions and plant diseases. This study aims to characterise climate change impacts on viticulture conditions accounting for training systems and cultivars likely to be found in major French wine-growing regions. The impact of the evolution of agro- and eco-climatic indices on the phenological stage was analysed for 8 cultivars, past and projected 8 km gridded climate data from 19 GCM with two SSP emission scenarios over 21 wine-growing regions.

It is, to our knowledge, the first systematic analysis performed over most regions of a major wine-producing country. Results suggest that the expected increased temperature will speed up grapevine development, favour flowering and might induce more heat damage in all wine regions, especially under Mediterranean climate conditions. Precipitation will probably decrease during the growing season. The southwestern part of France could be the most affected. This decrease would mainly occur during the grape ripening period, leading to a higher water deficit stress combined with higher temperatures. The spread between GCMs makes the changes in rainfall during the flowering stages of grapevine highly uncertain. According to our simulations, spring frost risk should remain stable in the future. However, the high sensibility of the output depending on the phenology model used induces a high level of uncertainty.

ACKNOWLEDGEMENTS

The authors thank Météo-France for their collaboration in providing access to SIM gridded data. We are grateful to the computing center at the University of Burgundy, which enabled us to carry out all the computer calculations. We also thank Basile Pauthier (CIVC) for providing useful information concerning viticulture and climate change in Champagne.

REFERENCES

Ausseil, A.-G. E., Law, R. M., Parker, A. K., Teixeira, E. I., & Sood, A. (2021). Projected Wine Grape Cultivar Shifts Due to Climate Change in New Zealand. *Frontiers in Plant Science*, *12*. https://www.frontiersin.org/articles/10.3389/fpls.2021.618039

Bécart, V., Lacroix, R., Puech, C., & Cortázar-Atauri, I. G. de. (2022). Assessment of changes in Grenache grapevine maturity in a Mediterranean context over the last half-century. *OENO One*, *56*(1), 53-72. https://doi.org/10.20870/oeno-one.2022.56.1.4727

Bois, B. (2007). *Cartographie agroclimatique à méso-échelle : Méthodologie et application à la variabilité spatiale du climat en Gironde viticole. Conséquences pour le développement de la vigne et la maturation du raisin.* [PhD Thesis]. Université Bordeaux 2.

Bonnefoy, C. (2013). *Observation et modélisation spatiale de la température dans les terroirs viticoles du Val de Loire dans le contexte du changement climatique* [Thèse de doctorat, Rennes 2]. https://www.theses.fr/2013REN20015

Caffarra, A., & Eccel, E. (2010). Increasing the robustness of phenological models for *Vitis vinifera* cv. Chardonnay. *International Journal of Biometeorology*, *54*(3), 255-267. https://doi.org/10.1007/s00484-009-0277-5

Caubel, J., García de Cortázar-Atauri, I., Launay, M., de Noblet-Ducoudré, N., Huard, F., Bertuzzi, P., & Graux, A.-I. (2015). Broadening the scope for ecoclimatic indicators to assess crop climate suitability according to ecophysiological, technical and quality criteria. *Agricultural and Forest Meteorology*, *207*, 94106. https://doi.org/10.1016/j.agrformet.2015.02.005

Chuine, I., Yiou, P., Viovy, N., Seguin, B., Daux, V., & Ladurie, E. L. R. (2004). Grape ripening as a past climate indicator. *Nature*, *432*, 289-290. https://doi.org/10.1038/432289a

Chuine, I., Bonhomme, M., Legave, J.-M., Cortázar-Atauri, I. G. de, Charrier, G., Lacointe, A., & Améglio, T. (2016). Can phenological models predict tree phenology accurately in the future? The unrevealed hurdle of endodormancy break. *Global Change Biology*, *22*(10), 3444-3460. https://doi.org/10.1111/gcb.13383

Cuccia, C. (2013). *Impacts du changement climatique sur la phénologie du Pinot noir en Bourgogne* [PhD Thesis]. Université de Bourgogne.

Daux, V., Garcia de Cortazar-Atauri, I., Yiou, P., Chuine, I., Garnier, E., Le Roy Ladurie, E., Mestre, O., & Tardaguila, J. (2012). An open-access database of grape harvest dates for climate research: Data description and quality assessment. *Climate of the Past*, *8*(5), 1403-1418. https://doi.org/10.5194/cp-8-1403-2012

de Rességuier, L., Mary, S., Le Roux, R., Petitjean, T., Quénol, H., & van Leeuwen, C. (2020). Temperature variability at local scale in the Bordeaux area. Relations with environmental factors and impact on vine phenology. *Frontiers in Plant Science*, *11*. https://doi.org/10.3389/fpls.2020.00515

Droulia, F., & Charalampopoulos, I. (2021). Future climate change impacts on European viticulture: a review on recent scientific advances. *Atmosphere*, *12*(4), 495. https://doi.org/10.3390/atmos12040495

Duchène, E., & Schneider, C. (2005). Grapevine and climatic changes: A glance at the situation in Alsace. *Agronomy for Sustainable Development*, *25*(1), 93-99. https://doi.org/10.1051/agro:2004057

Eyring, V., Bony, S., Meehl, G. A., Senior, C. A., Stevens, B., Stouffer, R. J., and Taylor, K. E. (2016). Overview of the Coupled Model Intercomparison Project Phase 6 (CMIP6) experimental design and organization, *Geoscientific Model Development*, 9(5), 1937–1958, https://doi.org/10.5194/gmd-9-1937-2016

García de Cortázar-Atauri, I., Brisson, N., & Gaudillere, J. P. (2009). Performance of several models for predicting budburst date of grapevine (*Vitis vinifera* L.). *International Journal of Biometeorology*, *53*(4), 317-326. https://doi.org/10.1007/s00484-009-0217-4

García de Cortázar-Atauri, I., Daux, V., Garnier, E., Yiou, P., Viovy, N., Seguin, B., Boursiquot, J. M., Parker, A. K., van Leeuwen, C., & Chuine, I. (2010). Climate reconstructions from grape harvest dates: Methodology and uncertainties. *The Holocene*, *20*(4), 599-608. https://doi.org/10.1177/0959683609356585

García de Cortázar-Atauri, I., Duchêne, E., Destrac-Irvine, A., Barbeau, G., Rességuier, L. de, Lacombe, T., Parker, A. K.,

Saurin, N., & van Leeuwen, C. (2017). Grapevine phenology in France: From past observations to future evolutions in the context of climate change. *OENO One*, *51*(2), 115-126. https://doi.org/10.20870/oeno-one.2017.51.2.1622

Gavrilescu, C., Zito, S., Richard, Y., Castel, T., Morvan, G., & Bois, B. (2022). *Frost risk projections in a changing climate are highly sensitive in time and space to frost modelling approaches*. XIVth International Terroir Congress and 2nd ClimWine Symposium, 3-8 July 2022, Bordeaux, France.

Gudmundsson, L., Bremnes, J. B., Haugen, J. E., & Engen-Skaugen, T. (2012). Technical Note: Downscaling RCM precipitation to the station scale using statistical transformations & ndash; a comparison of methods. *Hydrology and Earth System Sciences*, *16*(9), 3383-3390. https://doi.org/10.5194/hess-16-3383-2012

Joly, D., Brossard, T., Cardot, H., Cavailhes, J., Hilal, M., & Wavresky, P. (2010). Les types de climats en France, une construction spatiale. *Cybergeo : European Journal of Geography*. https://doi.org/10.4000/cybergeo.23155

Jones, G. V. (2003). Climate and terroir: Impacts of climate variability and change on wine. *Elements*, *14*(3), 167-172. https://doi.org/10.2138/gselements.14.3.167

Jones, G. V., Duchêne, E., Tomasi, D., Yuste, J., Braslavska, O., Martinez, C., Boso, S., Langellier, F., & Perruchot, C. (2005). *Changes in European winegrape phenology and relationships with climate*. 9.

Labbé, T., Pfister, C., Brönnimann, S., Rousseau, D., Franke, J., & Bois, B. (2019). The longest homogeneous series of grape harvest dates, Beaune 1354–2018, and its significance for the understanding of past and present climate. *Climate of the Past*, *15*(4), 14851501. https://doi.org/10.5194/cp-15-1485-2019

Lebon, E., Dumas, V., Pieri, P., & Schultz, H. R. (2003). Modelling the seasonal dynamics of the soil water balance of vineyards. *Functional Plant Biology*, *30*, 699710.

Martínez-Lüscher, J., Kizildeniz, T., Vučetić, V., Dai, Z., Luedeling, E., van Leeuwen, C., Gomès, E., Pascual, I., Irigoyen, J. J., Morales, F., & Delrot, S. (2016). Sensitivity of Grapevine Phenology to Water Availability, Temperature and CO2 Concentration. *Frontiers in Environmental Science*, *4*. https://www.frontiersin.org/articles/10.3389/fenvs.2016.00048

Menzel, A., Sparks, T. H., Estrella, N., Koch, E., Aasa, A., Ahas, R., Alm-Kübler, K., Bissolli, P., Braslavská, O., Briede, A., Chmielewski, F. M., Crepinsek, Z., Curnel, Y., Dahl, Å., Defila, C., Donnelly, A., Filella, Y., Jatczak, K., Måge, F., … Zust, A. (2006). European phenological response to climate change matches the warming pattern. *Global Change Biology*, 12(10). https://doi.org/10.1111/j.1365-2486.2006.01193.x

Molitor, D., Junk, J., Evers, D., Hoffmann, L., & Beyer, M. (2014). A High-Resolution Cumulative Degree Day-Based Model to Simulate Phenological Development of Grapevine. *American Journal of Enology and Viticulture*, 65(1), 72-80. https://doi.org/10.5344/ajev.2013.13066

Molitor, D., Fraga, H., & Junk, J. (2020). UniPhen – a unified high resolution model approach to simulate the phenological development of a broad range of grape cultivars as well as a potential new bioclimatic indicator. *Agricultural and Forest Meteorology*, 291, 108024. https://doi.org/10.1016/j.agrformet.2020.108024

Morales-Castilla, I., García de Cortázar-Atauri, I., Cook, B. I., Lacombe, T., Parker, A., van Leeuwen, C., Nicholas, K. A., & Wolkovich, E. M. (2020). Diversity buffers winegrowing regions from climate change losses. *Proceedings of the National Academy of Sciences*, *117*(6), 2864-2869. https://doi.org/10.1073/pnas.1906731117

Morinaga, K., Yakushiji, H., Koshita, Y., & Imai, S. (2000). Effect of fruit load levels on root activity, vegetative growth and sugar accumulation in berries of grapevine. *Acta Hort.*, *512*, 121128.

Ollat, N., Zito, S., Richard, Y., Aigrain, P., Brugière, F., Duchêne, E., Cortazar-Atauri, I. G. D., Gautier, J., Giraud-Héraud, E., Hannin, H., Touzard, J.-M., & Bois, B. (2021). La diversité des vignobles français face au changement climatique : Simulations climatiques et prospective participative. *Climatologie*, *18*, 3. https://doi.org/10.1051/climat/202118003

Palliotti, A., Tombesi, S., Silvestroni, O., Lanari, V., Gatti, M., & Poni, S. (2014). Changes in vineyard establishment and canopy management urged by earlier climate-related grape ripening: A review. *Scientia Horticulturae*, *178*, 4354. https://doi.org/10.1016/j.scienta.2014.07.039

Parker, A., García de Cortázar-Atauri, I., Gény, L., Spring, J.-L., Destrac, A., Schultz, H., Molitor, D., Lacombe, T., Graça, A., Monamy, C., Stoll, M., Storchi, P., Trought, M. C. T., Hofmann, R. W., & van Leeuwen, C. (2020). Temperature-based grapevine sugar ripeness modelling for a wide range of *Vitis vinifera* L. cultivars. *Agricultural and Forest Meteorology*, *285286*, 107902. https://doi.org/10.1016/j.agrformet.2020.107902

Parker, A., García de Cortázar-Atauri, I., van Leeuwen, C., & Chuine, I. (2011). General phenological model to characterise the timing of flowering and veraison of *Vitis vinifera* L. *Australian Journal of Grape and Wine Research*, *17*(2), 206-216. https://doi.org/10.1111/j.1755-0238.2011.00140.x

Rajha, H. N., Darra, N. E., Kantar, S. E., Hobaika, Z., Louka, N., & Maroun, R. G. (2017). A Comparative Study of the Phenolic and Technological Maturities of Red Grapes Grown in Lebanon. *Antioxidants*, *6*(1), 8. https://doi.org/10.3390/antiox6010008

Riou, C., Valancogne, C., & Pieri, P. (1989). Un modèle simple d'interception du rayonnement solaire par la vigne - vérification expérimentale. Agronomie, 1989, 9 (5),441-450. https://doi.org/10.1051/agro:19890502

Sgubin, G., Swingedouw, D., Dayon, G., García de Cortázar-Atauri, I., Ollat, N., Pagé, C., & van Leeuwen, C. (2018). The risk of tardive frost damage in French vineyards in a changing climate. *Agricultural and Forest Meteorology*, *250251*, 226242. https://doi.org/10.1016/j.agrformet.2017.12.253

Sgubin, G., Swingedouw, D., Mignot, J., Gambetta, G. A., Bois, B., Loukos, H., Noël, T., Pieri, P., García de Cortázar-Atauri, I., Ollat, N., & van Leeuwen, C. (2023). Non-linear loss of suitable wine regions over Europe in response to increasing global warming. *Global Change Biology*, *29*(3), 808826. https://doi.org/10.1111/gcb.16493

Simonovici, M. (2019). Enquête Pratiques phytosanitaires en viticulture en 2016. *Agreste Les Dossiers*, *20192*.

van Leeuwen, C., & Destrac-Irvine, A. (2017). Modified grape composition under climate change conditions requires adaptations in the vineyard. *OENO One*, *51*(2), 147-154. https://doi.org/10.20870/oeno-one.2017.51.2.1647

van Leeuwen, C., & Darriet, P. (2016). The Impact of Climate Change on Viticulture and Wine Quality. *Journal of Wine Economics*, *11*(1), 150-167. https://doi.org/10.1017/jwe.2015.21

van Leeuwen, C., Barbe, J.-C., Darriet, P., Destrac-Irvine, A., Gowdy, M., Lytra, G., Marchal, A., Marchand, S., Plantevin, M., Poitou, X., Pons, A., & Thibon, C. (2022). Aromatic maturity is a cornerstone of terroir expression in red wine. XIVth International Terroir Congress and 2nd ClimWine Symposium, 3-8 July 2022, Bordeaux, France. *OENO One*, *56*(2). https://doi.org/10.20870/oeno-one.2022.56.2.5441

Vidal, J.-P., Martin, E., Franchistéguy, L., Baillon, M., & Soubeyroux, J.-M. (2010). A 50-year high-resolution

atmospheric reanalysis over France with the Safran system. *International Journal of Climatology*, 30(11), 1627-1644. https://doi.org/10.1002/joc.2003

Webb, L. b., Whetton, P. h., & Barlow, E. w. r. (2007). Modelled impact of future climate change on the phenology of winegrapes in Australia. *Australian Journal of Grape and Wine Research*, *13*(3), 165175. https://doi.org/10.1111/j.1755-0238.2007.tb00247.x

Webb, L. B., Whetton, P. H., Bhend, J., Darbyshire, R., Briggs, P. R., & Barlow, E. W. R. (2012). Earlier wine-grape ripening driven by climatic warming and drying and management practices. *Nature Climate Change*, *2*(4), 259-264. https://doi.org/10.1038/nclimate1417

Wolfe, D. W., Schwartz, M. D., Lakso, A. N., Otsuki, Y., Pool, R. M., & Shaulis, N. J. (2005). Climate change and shifts in spring phenology of three horticultural woody perennials in northeastern USA. *International Journal of Biometeorology*, *49*(5). https://doi.org/10.1007/s00484-004-0248-9

Zito, S. (2021). *Evolution du risque phytosanitaire au vignoble dans le nord-est de la France en lien avec le changement climatique : Observations et modélisation : Cas de l'oïdium de la vigne* [Thèse de doctorat, Bourgogne Franche-Comté]. http://www.theses.fr/2021UBFCK033